ADP-14-22/T880

Dispersive estimate of the electromagnetic charge symmetry violation in the octet baryon masses

F. B. Erben,[1,2] P. E. Shanahan,[1] A. W. Thomas,[1] and R. D. Young[1]

[1] *CSSM & CoEPP, Department of Physics, University of Adelaide, Adelaide SA 5005, Australia*
[2] *Institut für Kernphysik, Becher-Weg 45, University of Mainz, D-55099 Mainz, Germany*

We explore the electromagnetic contribution to the charge symmetry breaking in the octet baryon masses using a subtracted dispersion relation based on the Cottingham formula. For the proton–neutron mass splitting we report a minor revision of the recent analysis of Walker-Loud, Carlson and Miller. For the electromagnetic structure of the hyperons we constrain our analysis, where possible, by a combination of lattice QCD and SU(3) symmetry breaking estimates. The results for the baryon mass splittings are found to be compatible with recent lattice QCD+QED determinations. The uncertainties in the dispersive analysis are dominated by the lack of knowledge of the hyperon inelastic structure.

arXiv:1408.6628v1 [nucl-th] 28 Aug 2014

I. INTRODUCTION

A vast array of nuclear and hadronic physics processes are almost invariant under charge symmetry [1, 2]. As a result, the assumption of good charge symmetry has been widely applied in nuclear and strong interaction studies. With the description of strong interaction phenomena in terms of the fundamental theory of quantum chromodynamics (QCD) progressing into the precision era, it is now essential to further quantify the degree to which charge symmetry is violated — see for example the search for new physics in β decays [3]. Charge symmetry violation (CSV) is driven by two sources, that arising from the inequality of the light-quark masses ($m_u \neq m_d$), which we will refer to as the strong component, and that arising from the electromagnetic interaction.

The prime example of charge symmetry violation (CSV) is the observed $\sim 0.1\%$ difference in the masses of the proton and neutron. Calculations in lattice QCD have recently made significant advances in the determination of the strong component of this mass difference [4–9]. In parallel, the theoretical description of the electromagnetic contribution has been improved by the work of Walker-Loud, Carlson & Miller (WCM) [10] using a new formulation of the Cottingham formula [11]. Lattice QCD+QED [5, 9, 12] is also making progress in the direct calculation of the electromagnetic contribution.

The principal focus of the present work is the extension of the WCM dispersive analysis to investigate the electromagnetic contribution to the mass splittings of the Σ and Ξ baryons. The theoretical inputs required for the dispersion integral are described in terms of the electromagnetic structure, for which very little is known phenomenologically for the hyperons. The results presented here utilise input from lattice QCD, where available, with conservative estimates of the magnitude of SU(3) breaking effects applied elsewhere.

In his seminal work [11], Cottingham showed that the electromagnetic self-energies of the nucleons can be computed in terms of the imaginary part of the forward Compton amplitude, which is measurable in inclusive electron–nucleon scattering experiments. Using the Cottingham result, the long-standing accepted value for the electromagnetic contribution to the proton-neutron mass splitting was $\delta M^{\gamma}_{p-n} = 0.76 \pm 0.30\,\text{MeV}$ [13, 14]. The recent work of WCM has challenged this result by demonstrating that the application of the Cottingham formula with two different Lorentz decompositions of the Compton scattering tensor leads to incompatible results [10]. By using a subtracted dispersive analysis, WCM demonstrated that this ambiguity can be removed. The revised value of the dispersive estimate of the electromagnetic mass splitting was reported to be $\delta M^{\gamma}_{p-n} = 1.30 \pm 0.47\,\text{MeV}$ [10]. An extension of the WCM formalism [15] which incorporates quark-mass dependence and finite volume effects, combined with the lattice simulation results of Ref. [5], provides an improved constraint on the dispersion integral $\delta M^{\gamma}_{p-n} = 1.04 \pm 0.11\,\text{MeV}$.

II. ELECTROMAGNETIC SELF-ENERGY

As described by WCM, the use of a subtracted dispersion relation for the determination of the electromagnetic self-energy of a baryon B leads to the natural separation of contributions given by

$$\delta M^{\gamma}_B = \delta M^{\text{el}}_B + \delta M^{\text{inel}}_B + \delta M^{\text{sub}}_B + \delta \tilde{M}^{\text{ct}}_B \,. \qquad (1)$$

In the following subsections, each of these contributions is examined in the light of our current understanding of nucleon and hyperon structure.

A. Elastic

The elastic contribution to the self-energy is given by

$$\delta M^{\text{el}}_B = \frac{\alpha}{\pi}\int_0^{\Lambda_0} dQ \Bigg[\frac{3}{2} G_M^2 \frac{\sqrt{\tau_{\text{el}}}}{\tau_{\text{el}}+1} + (G_E^2 - 2\tau_{\text{el}} G_M^2)\frac{(1+\tau_{\text{el}})^{3/2} - \tau_{\text{el}}^{3/2} - \frac{3}{2}\sqrt{\tau_{\text{el}}}}{\tau_{\text{el}}+1}\Bigg], \qquad (2)$$

with $\tau_{\rm el} = Q^2/(4M_B^2)$. G_E and G_M represent the electric and magnetic Sachs form factors of the corresponding baryon. For the proton and neutron, these are rather well-known empirically and we make use of the Kelly parameterisation [16] of experimental results. The upper limit of integration, Λ_0, denotes the scale at which perturbative evolution becomes reliable. We follow WCM by reporting central estimates using $\Lambda_0^2 = 2\,{\rm GeV}^2$, and uncertainties calculated by allowing for variation over the range $1.5 < \Lambda_0^2 < 2.5\,{\rm GeV}^2$ [10].

For the hyperons, we use lattice-QCD-based results from the CSSM/QCDSF/UKQCD Collaborations. The lattice study of Refs. [17, 18] presents results for the electromagnetic form factors of all outer-ring octet baryons at a range of discrete values of the momentum transfer, Q^2. The analysis includes finite-volume corrections and a chiral extrapolation to the physical pseudoscalar masses. In addition, simple parameterizations of the Q^2-dependence of the form factors are given at the physical point. It is these parameterizations which we use here.

It was found in Ref. [18], for the electric form factors, that standard dipole parameterizations of the Q^2-dependence of G_E perform poorly. Here, for the charged baryons, we use the more general fits presented in that work,

$$G_{E,\rm fit}^B(Q^2) = \frac{G_E^B(Q^2=0)}{1 + c_1 Q^2 + c_2 Q^4 + c_3 Q^6}. \qquad (3)$$

For the neutral cascade baryon form factor, where the charge $G_E^{\Xi^0}(Q^2=0) = 0$, we use the same form, fit to the individual quark-sector contributions to the form factor. The total form factor is then deduced as

$$G_E^{\Xi^{0/-}} = \mathcal{Q}_{u/d} G_{E,\rm fit}^{\Xi^0,u}(Q^2) + 2\mathcal{Q}_s G_{E,\rm fit}^{\Xi^0,s}(Q^2)\,, \qquad (4)$$

with $\mathcal{Q}_{u,d,s}$ the charges of the respective quarks. For consistency this same process is followed for the Ξ^-.

Similarly, we take parameterizations of the hyperon magnetic form factors from Ref. [17]. The function that best reproduced the lattice simulation results is

$$G_{M,\rm fit}^B(Q^2) = \frac{\mu_B}{1 + c_1 Q^2 + c_2 Q^4 + c_3 Q^6}, \qquad (5)$$

where μ_B denotes the experimental value of the magnetic moment of the baryon B [19]. Here, as in Ref. [17], G_M has been expressed in units of the nuclear magneton $\mu_{\rm N} \equiv e\hbar/(2M_p)$. Note that in order to use these expressions in Eq. (2) one must multiply them by a factor M_B/M_p. The elastic contributions to the mass splittings are summarised in Table I.

B. Inelastic

The inelastic contribution to the electromagnetic self-energy can be expressed in the form

$$\delta M_B^{\rm inel} = \int_{W_0^2}^{\infty} dW^2\, \Omega_B^{\rm inel}(W^2), \qquad (6)$$

where

$$\Omega^{\rm inel}(W^2) = \frac{\alpha}{\pi}\int_0^{\Lambda_0} dQ \Bigg\{ \frac{3F_1(W^2,Q^2)}{4M_B^2}\,\frac{2\tau^{\frac{3}{2}} - 2\tau\sqrt{1+\tau} + \sqrt{\tau}}{\tau} + \frac{F_2(W^2,Q^2)}{(Q^2+W^2-M_B^2)}\left[(1+\tau)^{\frac{3}{2}} - \tau^{\frac{3}{2}} - \tfrac{3}{2}\sqrt{\tau}\right]\Bigg\} \qquad (7)$$

with $\tau = (W^2+Q^2-M_B^2)^2/(4M_B^2Q^2)$ and $W_0 = (M_B + m_\pi)$. F_1 and F_2 denote the baryon inelastic structure functions. We note that the standard derivation of the dispersion integral yields an integral with respect to ν, the energy transferred to the target. Here we have transformed the integration variable $\nu \to W^2$, where W^2 is the invariant mass-squared of the hadronic intermediate state, in order to highlight the distinct resonance structures.

The structure functions F_1 and F_2 have been measured extensively for the proton and deuteron. For the low to intermediate W region we make use of the parameterisations of Christy & Bosted (CB) [20, 21]. As nearly all data points agree with the proton structure function parameterisations to better than 5%, we take the conservative estimate of a uniform 5% uncertainty in $F_{1,2}^p$. The parameterisation of the deuteron scattering data is in similar agreement at the 3–5% level [20], with some data points out to ∼10% disagreement in limited kinematic domains. Since the neutron structure functions are estimated by subtracting out the knowledge of the proton, we assign a conservative 10% uncertainty on the neutron structure functions.

Figure 1 displays the integrand $\Omega_{p-n}^{\rm inel}(W^2)$ contributing to the proton–neutron mass splitting calculated using the CB parameterisations. Under exact charge symmetry, the cross sections for $\gamma^* p \to \Delta^+$ and $\gamma^* n \to \Delta^0$ are identical. The central values of the Bosted & Christy parameterisation give a violation of this symmetry by about 18% in the Delta production rate. This significant CSV effect is what causes the large dip structure seen in Fig. 1 in the Delta region. While we expect some CSV in the Delta region the CB value seem excessively large. Bearing in mind that such effects are inextricably linked with the extraction of the photo-neutron cross section for the deuteron, in the present analysis we prefer to take a charge symmetric Delta production rate as our central value. To achieve this, we set the Delta parameters of the Bosted-Christy deuteron fits to match those of the proton results. We attach a 100% uncertainty to this artificial modification of the empirical fits. This modification leads to an appreciable change in the cross sections only in the difficult-to-constrain low-Q and low-W region. As a consequence of restoring charge symmetry to the Delta region, the central value of $\delta M_{p-n}^{\rm inel}$ is increased by just 0.020 MeV.

For the region $W^2 > 9\,{\rm GeV}^2$ we use the Regge form for the inelastic structure functions proposed by Capella et

TABLE I. Decomposition of the electromagnetic contributions to the octet baryon mass splittings as defined in Eq. (1).

Baryon	$\delta M^{\rm el}$	$\delta M^{\rm inel}$	$\delta M^{\rm sub}_{\rm el}$	$\delta M^{\rm sub}_{\rm inel}$	$\delta \tilde{M}^{\rm ct}$	δM^{γ}
$p-n$	1.401(7)	0.089(42)	−0.635(7)	0.18(35)	0.006	1.04(35)
$\Sigma^+ - \Sigma^-$	1.24(7)	0.02(21)	−1.89(10)	0.6(11)	0.014(1)	0.0(11)
$\Xi^0 - \Xi^-$	−0.636(30)	0.42(15)	−0.80(4)	0.6(11)	0.008	−0.4(11)

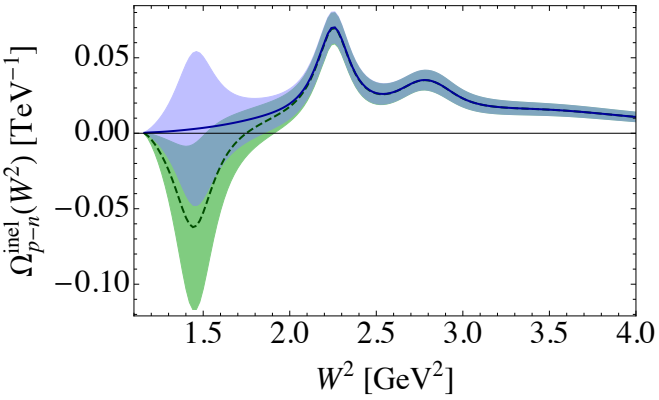

FIG. 1. The integrand (with respect to W^2) of the inelastic dispersion integral contributing to the $p-n$ electromagnetic self-energy (shown for $\mu^2 = 2\,\text{GeV}^2$). The dotted line shows the result of the direct application of the Bosted-Christy structure functions. The solid line shows the same quantity where the Delta resonance contribution has been forced to be isospin symmetric. In both cases the shaded regions reflect a characteristic uncertainty in the parameterisations of the individual structure functions.

al. [22], with the modifications summarised by Sibirtsev et al. [23].

In summary, we determine the inelastic contributions to the dispersion integral for the nucleons to be

$$\delta M_p^{\rm inel} = 0.62 \pm 0.03 \pm 0.07, \tag{8}$$
$$\delta M_n^{\rm inel} = 0.53 \pm 0.05 \pm 0.05, \tag{9}$$
$$\delta M_{p-n}^{\rm inel} = 0.089 \pm 0.038 \pm 0.019, \tag{10}$$

where the first error is that from the uncertainty associated with the structure functions and the second is from the range of Λ_0^2.

Very little is known experimentally about the hyperon structure functions. There are some older studies based on the MIT bag model [24], while recent lattice QCD studies have provided insight into the partonic structure of the octet baryons [25, 26]. These simulations offer some guidance as to the size of SU(3) breaking effects in the inelastic structure functions. Based on the results of a recent chiral extrapolation [27], we report estimates for the ratios of the quark momentum fractions at the physical quark masses:

$$R_u^\Sigma \equiv \frac{\langle x\rangle_u^\Sigma}{\langle x\rangle_u^p} = 1.2(1), \quad R_d^\Sigma \equiv \frac{\langle x\rangle_s^\Sigma}{\langle x\rangle_d^p} = 1.5(1), \tag{11}$$
$$R_u^\Xi \equiv \frac{\langle x\rangle_s^\Xi}{\langle x\rangle_u^p} = 1.19(4), \quad R_d^\Xi \equiv \frac{\langle x\rangle_u^\Xi}{\langle x\rangle_d^p} = 1.4(2). \tag{12}$$

While the partonic interpretation is not generally applicable at the low-Q^2 values of relevance to the integral of Eq. (7), we will adopt the flavour separation to enable us to use these lattice estimates, Eqs. (11) & (12), to guide the significance of the SU(3) breaking. We write the up or down contributions to the nucleon structure functions in terms of the proton and neutron structure functions as

$$F^{N,u} = \frac{9}{15}\left(4F^p - F^n\right), \quad F^{N,d} = \frac{9}{15}\left(4F^n - F^p\right). \tag{13}$$

Here we have assumed partonic charge symmetry, i.e., $F^{N,u} \equiv F^{p,u} = F^{n,d}$ and $F^{N,d} \equiv F^{p,d} = F^{n,u}$. To estimate the inelastic self-energies of Eq. (7) we use structure functions that are scaled by the lattice estimates

$$F^{\Sigma,u} \simeq \frac{\langle x\rangle_u^\Sigma}{\langle x\rangle_u^p} F^{N,u}, \quad F^{\Sigma,s} \simeq \frac{\langle x\rangle_s^\Sigma}{\langle x\rangle_d^p} F^{N,d}, \tag{14}$$
$$F^{\Xi,s} \simeq \frac{\langle x\rangle_s^\Xi}{\langle x\rangle_u^p} F^{N,u}, \quad F^{\Xi,u} \simeq \frac{\langle x\rangle_u^\Xi}{\langle x\rangle_d^p} F^{N,d}. \tag{15}$$

We caution that the resonance structures in the hyperons are markedly different from those in the nucleons. Nevertheless, the success of duality in the case of the nucleon [28] suggests that such W^2-integrated quantities may be reasonably estimated by this simple SU(3) scaling. This assumption could be improved upon with a more thorough analysis of the flavour separation in the low-Q^2 region, such as that explored in Refs. [29–31]. Given the relatively small magnitude of $\delta M^{\rm inel}$, such an improvement is not warranted in the present calculation.

Under the assumptions stated previously, we can estimate the hyperon inelastic integrals in terms of the corresponding nucleon results. Explicitly,

$$\delta M^{\rm inel}_{\Sigma^+-\Sigma^-} = \left(\mathcal{Q}_u^2 - \mathcal{Q}_d^2\right)\frac{9}{15} R_u^\Sigma \left(4\delta M_p^{\rm inel} - \delta M_n^{\rm inel}\right), \tag{16}$$

$$\delta M^{\rm inel}_{\Xi^0-\Xi^-} = \left(\mathcal{Q}_u^2 - \mathcal{Q}_d^2\right)\frac{4}{15} R_d^\Xi \left(4\delta M_n^{\rm inel} - \delta M_p^{\rm inel}\right). \tag{17}$$

For a conservative estimate of the uncertainties, we include an uncertainty on the lattice momentum fraction ratios (R_q^B) that allows for a 100% variation of the amount of SU(3) violation (i.e. $R_q^B - 1$). The final results for the hyperon inelastic integrals are summarised in Table I.

C. Subtraction

Using the subtracted dispersion formalism of WCM, one is left with a dependence of the self-energy on the real part of the forward Compton amplitude evaluated at $\nu = 0$ [10]

$$\delta M_B^{\rm sub} = -\frac{3\alpha}{16\pi M_B}\int_0^{\Lambda_0^2} dQ^2\, T_1^B(0,Q^2), \qquad (18)$$

(see Ref. [10] for the Lorentz decomposition of the Compton amplitude). The amplitude $T_1(0,Q^2)$ has received considerable attention recently [32–34] in relation to the proton radius puzzle [35, 36]. Knowledge of the momentum dependence of T_1 can be expressed as

$$T_1^B(0,Q^2) = 2G_M^2(Q^2) - 2F_D^2(Q^2) + Q^2\frac{2M_B}{\alpha}\beta_M^B F_\beta(Q^2), \qquad (19)$$

where F_D denotes the elastic Dirac form factor. The first two terms in this expression can naturally be described as the elastic contribution. This contribution to the self-energy,

$$\delta M_{\rm el}^{\rm sub} = -\frac{3\alpha}{16\pi M}\int_0^{\Lambda_0^2} dQ^2\left[2G_M^2(Q^2) - 2F_D^2(Q^2)\right] \qquad (20)$$

is readily evaluated using the form factors described above. The results are displayed in Table I.

The final term in Eq. (19) describes an inelastic component, which, as in the calculation of WCM, constitutes the dominant uncertainty in the calculation. In a small-Q^2 expansion of this component the leading term is given by the magnetic polarisability [37]. A recent phenomenological analysis of the nucleon magnetic polarizabilities has reported [38]

$$\beta_M^p = (3.1 \pm 0.8)\times 10^{-4}\,{\rm fm}^3, \qquad (21)$$

$$\beta_M^n = (4.1 \pm 2.0)\times 10^{-4}\,{\rm fm}^3, \qquad (22)$$

$$\beta_M^{p-n} = (-1.0 \pm 2.0)\times 10^{-4}\,{\rm fm}^3. \qquad (23)$$

Beyond leading order, the Q^2 dependence of the inelastic contribution is encoded in the form factor $F_\beta(Q^2)$. Using chiral perturbation theory, Birse and McGovern [34] have recently estimated that the small Q^2 behaviour of F_β for the proton may be described as

$$F_\beta = 1 + \frac{Q^2}{M_\beta^2} + \mathcal{O}(Q^4) \qquad (24)$$

with a mass scale

$$M_\beta = 460 \pm 100 \pm 40\,{\rm MeV}. \qquad (25)$$

At large Q^2, T_1 must fall like $1/Q^2$, as determined by the operator product expansion [39]. Collins has determined the coefficient of this dominant contribution at large Q^2 [39]:

$$T_1^B(0,Q^2) \overset{Q^2\to\infty}{=} \frac{1}{Q^2}\left\{4\kappa M_B^2 - 4\sum_q\left(\kappa + \mathcal{Q}_q^2\right)M_B\sigma_q^B + \mathcal{O}\left[\frac{1}{\log Q^2}\right]\right\}, \qquad (26)$$

where to lowest order in the strong coupling $\kappa = N_f/(33-2N_f)$, the sum is over N_f active flavours of quark q and σ_q^B denotes the sigma term for quark flavour q in baryon B. The flavour-dependent sigma terms, including charge symmetry violating effects, have been studied in recent lattice QCD analyses [7, 8]. The explicit flavour decomposition, based on the work reported in Refs. [8, 40, 41], is displayed in Table II.

To leading order in the isospin splittings, and still to first order in α (i.e., this term amounts to an $\mathcal{O}(\alpha(m_d - m_u))$ effect), only the isovector contribution is required and the large-Q^2 scaling can be written as

$$T_1^{\Delta B}(0,Q^2) \overset{Q^2\to\infty}{=} \frac{1}{Q^2}\left\{-4M_{\bar B}\left(\mathcal{Q}_u^2\frac{m_u}{\bar m} - \mathcal{Q}_d^2\frac{m_d}{\bar m}\right)\left(\sigma_u^{\bar B} - \sigma_d^{\bar B}\right) + \mathcal{O}\left[\frac{1}{\log Q^2}\right]\right\}, \qquad (27)$$

where we have introduced the isospin-averaged baryon masses $M_{\bar B}$ for $\bar B = \{N, \Sigma, \Xi\}$ and the light quark masses, m_u, m_d and $\bar m = (m_u + m_d)/2$. The isospin-averaged sigma terms are given by $\sigma_u^N = (\sigma_u^p + \sigma_d^n)/2$, $\sigma_d^N = (\sigma_d^p + \sigma_u^n)/2$, and similarly for the hyperon cases. Numerically, $T_1^{\Delta N}(0,Q^2)$ for the nucleon is of the order $(-2\times 10^{-3}\,{\rm GeV}^2)/Q^2$.

Given that the elastic form factors of the nucleon drop off at least as fast as $1/Q^2$, the elastic component in Eq. (19) is irrelevant to the large-Q^2 behaviour of

TABLE II. Flavour break down of light-quark sigma terms (all in MeV).

Baryon	p	n	Σ^+	Σ^-	Ξ^0	Ξ^-
σ_u^B	18(2)	14(1)	13.3(9)	3.8(6)	7.1(4)	1.3(2)
σ_d^B	26(3)	32(3)	7(1)	23(2)	2.4(4)	12.7(8)

$T_1(0,Q^2)$. Previous authors have advocated approximating F_β in the small [34] to intermediate [10] Q^2 region by a dipole form

$$F_\beta(Q^2) = \left(\frac{1}{1+Q^2/(2M_\beta^2)}\right)^2 . \tag{28}$$

While these authors have not suggested extending this form to asymptotically large Q^2, we note that this form does not give a consistent description of the leading $1/Q^2$ behaviour described above. Taking the central value for the nucleon isovector polarisability, $\beta_M^{p-n} \sim -1 \times 10^{-4}\,\mathrm{fm}^3$, in Eq. (19) with this dipole form and hadronic mass scale leads to a scaling behaviour $T_1^{\Delta N}(0,Q^2) \sim -0.8\,\mathrm{GeV}^2/Q^2$. This is a factor of ~ 400 larger than predicted by the operator product expansion.

To smoothly connect the small-Q^2 and asymptotic domains, we therefore suggest a model for the inelastic part of Eq. (19):

$$Q^2\frac{2M_{\bar B}}{\alpha}\beta_M^{\Delta B}F_\beta^{\Delta B}(Q^2) = \frac{Q^2 2M_{\bar B}\beta_M^{\Delta B}/\alpha + Q^4 C_{\Delta B}/(3M_\beta^2)^3}{(1+Q^2/(3M_\beta^2))^3}, \tag{29}$$

where $C_{\Delta B}$ is defined to describe exactly the dominant contribution to the operator product expansion dependence computed in Eq. (27). We note that because the coefficient $C_{\Delta B}$ is so small compared to the hadronic scale, it has no influence on the small-Q^2 expansion characterised by the mass scale M_β in Eq. (24).

Evaluation of the inelastic part of the subtraction term for the nucleon gives

$$\delta M_{\mathrm{inel}}^{p-n,\mathrm{sub}} = 0.18 \pm 0.35\,\mathrm{MeV}, \tag{30}$$

where the uncertainty reflects the limited knowledge of β_M^{p-n} and mass scale M_β. The quoted uncertainty range has been estimated by assuming β_M and $\log M_\beta$ to be normally distributed.

Polarizabilities of the hyperons are even less well known than those of the nucleon. A range of results have been obtained using a variety of theoretical approaches including chiral effective field theory [42]; soliton models [43]; $1/N_C$ expansions [44]; a computational hadronic model [45]; and lattice QCD [46]. In the present work we simply take the same value and uncertainty range for the isovector hyperon polarisabilities as quoted for the nucleon. The mass scale M_β associated with the hyperons has not been investigated. Since the physics is governed more considerably by the strange quarks, however, one may anticipate a harder scale than that for the nucleon. For this reason we take a more conservative range of mass scales for the hyperons, $M_\beta^{\Sigma,\Xi} = 0.7 \pm 0.3\,\mathrm{GeV}$. The resulting contributions to the sum rule are given by

$$\delta M_{\mathrm{inel}}^{\Sigma^+-\Sigma^-,\mathrm{sub}} = 0.6 \pm 1.1\,\mathrm{MeV}, \tag{31}$$

$$\delta M_{\mathrm{inel}}^{\Xi^0-\Xi^-,\mathrm{sub}} = 0.6 \pm 1.1\,\mathrm{MeV}. \tag{32}$$

As for the nucleon case, the uncertainties have been propagated assuming β_M and $\log M_\beta$ to be normally distributed.

D. Counter terms

The decompostion of the baryon mass splittings into electromagnetic and strong components is itself scale dependent. For sufficiently large Λ_0, where perturbative QCD is applicable, this scale dependence is entirely encoded in the operator product expansion analysis described above. Although the leading contributions are formally second order for the charge symmetry violating effects, we include them for completeness. This leading counterterm evaluates to

$$\delta\tilde{M}_{\Delta B}^{\mathrm{ct}} = -\frac{3\alpha}{16\pi M_{\bar B}} C_{\Delta B}\log\left(\frac{\Lambda_0^2}{\Lambda_1^2}\right), \tag{33}$$

where, following WCM, we have taken $\Lambda_0 = 2\,\mathrm{GeV}^2$ and $\Lambda_1^2 = 100\,\mathrm{GeV}^2$ for our numerical values, which are summarised in Table I.

III. TOTAL

In summary, our best estimates for the electromagnetic contribution to the baryon isospin mass splittings are

$$\delta M_{p-n}^\gamma = 1.04 \pm 0.35\,\mathrm{MeV}, \tag{34}$$

$$\delta M_{\Sigma^+-\Sigma^-}^\gamma = 0.0 \pm 1.1\,\mathrm{MeV}, \tag{35}$$

$$\delta M_{\Xi^0-\Xi^-}^\gamma = -0.4 \pm 1.1\,\mathrm{MeV}. \tag{36}$$

The value for the isospin breaking in the nucleon sector is compatible with the analysis by Walker-Loud et al. [10]. It is also in excellent agreement with the dispersion relation constrained by lattice QCD simulations [15].

In the hyperon sector, our findings compare favourably with lattice QCD+QED simulations from the BMW Collaboration [9]

$$\delta M_{p-n}^\gamma = 1.59 \pm 0.46\,\mathrm{MeV}, \tag{37}$$

$$\delta M_{\Sigma^+-\Sigma^-}^\gamma = 0.08 \pm 0.36\,\mathrm{MeV}, \tag{38}$$

$$\delta M_{\Xi^0-\Xi^-}^\gamma = -1.29 \pm 0.17\,\mathrm{MeV}. \tag{39}$$

As in the work of WCM, the uncertainty of the dispersion integral is dominated by the lack of knowledge

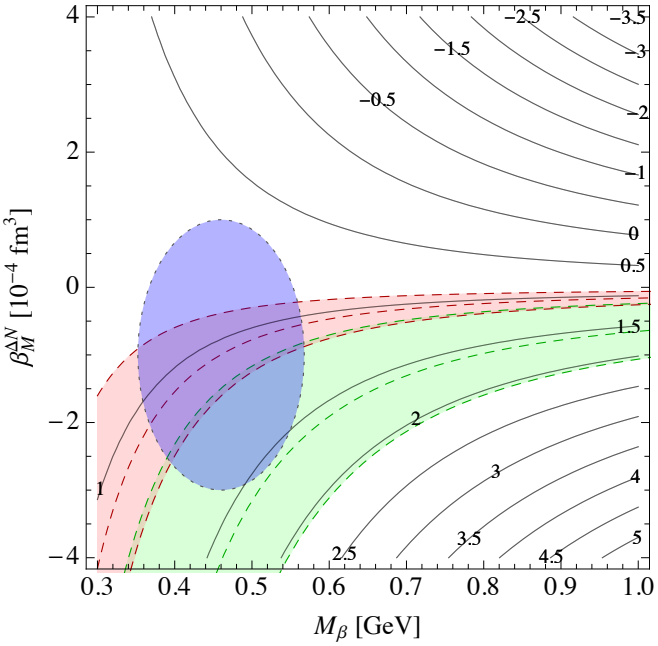

FIG. 2. The contours depict constant electromagnetic self-energy with respect to the dominant driving uncertainties, the isovector magnetic polarisability β_M^{p-n} and the mass parameter M_β (see Eq. (29)) characterising the mass scale by which the corresponding integral is suppressed. The contours are labelled in units of MeV, with the error bar on these lines implied at the level of ± 0.04 MeV. The blue ellipse denotes the best phenomenological estimates of these parameters as reported in Refs. [38] and [34], respectively. The shaded green band displays the lattice calculation of the electromagnetic self energy reported by the BMW Collaboration [9]. The red band shows the lattice-constrained dispersive estimate of δM^γ_{p-n} reported in Ref. [15].

of the inelastic subtraction term. Here we summarise the intermediate stage of the calculation, computing all contributions up to this isolated term:

$$\delta M^\gamma_{p-n} - \delta M^{p-n,\mathrm{sub}}_{\mathrm{inel}} = 0.86 \pm 0.04\,\mathrm{MeV}, \quad (40)$$

$$\delta M^\gamma_{\Sigma^+-\Sigma^-} - \delta M^{\Sigma^+-\Sigma^-,\mathrm{sub}}_{\mathrm{inel}} = -0.62 \pm 0.24\,\mathrm{MeV}, \quad (41)$$

$$\delta M^\gamma_{\Xi^0-\Xi^-} - \delta M^{\Xi^0-\Xi^-,\mathrm{sub}}_{\mathrm{inel}} = -1.00 \pm 0.16\,\mathrm{MeV}. \quad (42)$$

With these terms relatively well constrained, the lattice calculation of the total electromagnetic contribution allows us to explore the driving uncertainties in the inelastic subtraction term. Figure 2 displays the dependence of the nucleon electromagnetic mass splitting on the dominant uncertainties of the inelastic subtraction term. Compatibility between the dispersion calculation and lattice is observed. Unfortunately, given the present central values, it is difficult to improve the estimates for either β_M or M_β.

In Figure 3 we show similar comparison of the dispersion calculation with the lattice QCD+QED values of the electromagnetic mass differences. Even with the large range of Λ_β considered, it is evident the lattice results can

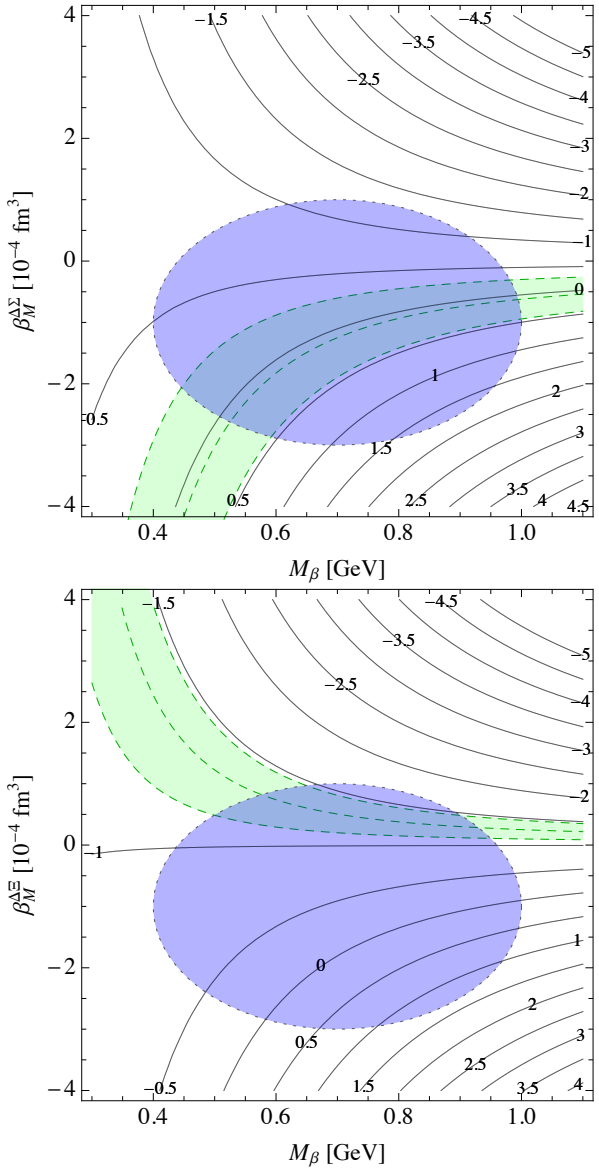

FIG. 3. Graph is labelled the same as Fig. 2, showing the sesitivity of the Σ (top panel) and Ξ (lower panel) baryon electromagnetic splittings to $\beta_M^{\Delta B}$ and M_β. Uncertainties on the black contours should be interpreted as ± 0.24 MeV for Σ and ± 0.16 MeV for Ξ.

play some meaningful constraint on the hyperon isovector polarisabilities. The figures suggest that $\beta_M^{\Sigma^+-\Sigma^-}$ lies in the range $(-3 \to 0)\cdot 10^{-4}$ fm^3 and $\beta_M^{\Xi^0-\Xi^-}$ in the range $(0 \to 1.5)\cdot 10^{-4}$ fm^3. If M_β turns out to be similarly soft, as suggested for the nucleon, then less restrictive bounds on the hyperon polarisabilities would result.

IV. SUMMARY

We have reported a new analysis of the Cottingham sum rule evaluation of the electromagnetic contribution

to mass differences in the octet baryon states. We have adapted the recently formulated subtracted dispersion approach introduced by Walker-Loud et al. to the hyperons, and implemented some minor updates for the proton-neutron system. Comparing with this earlier phenomenological work, the minor differences in the nucleon analysis arise from two sources: i) in this work, the significant CSV effects in the Delta region realised by the Bosted-Christy structure functions have been suppressed, this generates a rather small increase in the self energy; ii) the inelastic subtraction involving $T_1^{p-n}(0, Q^2)$ is suppressed more rapidly in this work in order to appropriately match onto the behaviour dictated by the operator product expansion. This acts to reduce the size of this term, and consequently lessen the sensitivity to the poorly-known isovector polarisability.

For the hyperons, the dispersive estimates have significantly larger uncertainties than for the nucleon, which are dominated by the lack of knowledge of the hyperon isovector polarisabilities. Comparison with recent lattice QCD+QED simulations suggests some modest bounds on the size of the isovector magnetic polarisabilities. Certainly further theoretical (or experimental) work on this aspect of hyperon structure would be of interest.

During the completion of this work, a new lattice QCD+QED study has been reported in Ref. [47]. While the results are compatible with those presented here, it is not clear that the choice of renormalisation scheme in that work is consistent with the Cottingham sum rule.

ACKNOWLEDGEMENTS

We thank Nathan Hall and James Zanotti for helpful conversations. This work was supported by the University of Adelaide and the Australian Research Council through the ARC Centre of Excellence for Particle Physics at the Terascale and grants FL0992247 (AWT), DP140103067, FT120100821 (RDY).

[1] G. A. Miller, A. K. Opper, and E. J. Stephenson, Ann.Rev.Nucl.Part.Sci. **56**, 253 (2006), arXiv:nucl-ex/0602021 [nucl-ex].
[2] J. T. Londergan, J. C. Peng, and A. W. Thomas, Rev.Mod.Phys. **82**, 2009 (2010), arXiv:0907.2352 [hep-ph].
[3] M. González-Alonso and J. Martin-Camalich, Phys.Rev.Lett. **112**, 042501 (2014), arXiv:1309.4434 [hep-ph].
[4] S. R. Beane, K. Orginos, and M. J. Savage, Nucl.Phys. **B768**, 38 (2007), arXiv:hep-lat/0605014 [hep-lat].
[5] T. Blum, R. Zhou, T. Doi, M. Hayakawa, T. Izubuchi, et al., Phys.Rev. **D82**, 094508 (2010), arXiv:1006.1311 [hep-lat].
[6] G. M. de Divitiis, P. Dimopoulos, R. Frezzotti, V. Lubicz, G. Martinelli, et al., JHEP **1204**, 124 (2012), arXiv:1110.6294 [hep-lat].
[7] R. Horsley et al. (QCDSF Collaboration, UKQCD Collaboration), Phys.Rev. **D86**, 114511 (2012), arXiv:1206.3156 [hep-lat].
[8] P. E. Shanahan, A. W. Thomas, and R. D. Young, Phys.Lett. **B718**, 1148 (2013), arXiv:1209.1892 [nucl-th].
[9] S. Borsanyi, S. Dürr, Z. Fodor, J. Frison, C. Hoelbling, et al., Phys.Rev.Lett. **111**, 252001 (2013), arXiv:1306.2287 [hep-lat].
[10] A. Walker-Loud, C. E. Carlson, and G. A. Miller, Phys.Rev.Lett. **108**, 232301 (2012), arXiv:1203.0254 [nucl-th].
[11] W. N. Cottingham, Annals Phys. **25**, 424 (1963).
[12] R. Horsley et al., PoS **Lattice2013**, 499 (2013), arXiv:1311.4554 [hep-lat].
[13] J. Gasser and H. Leutwyler, Nucl.Phys. **B94**, 269 (1975).
[14] J. Gasser and H. Leutwyler, Phys.Rept. **87**, 77 (1982).
[15] A. W. Thomas, X. G. Wang, and R. D. Young (2014), arXiv:1406.4579 [nucl-th].
[16] J. J. Kelly, Phys.Rev. **C70**, 068202 (2004).
[17] P. E. Shanahan et al., Phys.Rev. **D89**, 074511 (2014), arXiv:1401.5862 [hep-lat].
[18] P. E. Shanahan et al., Phys.Rev. **D90**, 034502 (2014), arXiv:1403.1965 [hep-lat].
[19] J. Beringer et al. (Particle Data Group), Phys.Rev. **D86**, 010001 (2012).
[20] M. E. Christy and P. E. Bosted, Phys.Rev. **C81**, 055213 (2010), arXiv:0712.3731 [hep-ph].
[21] P. E. Bosted and M. E. Christy, Phys.Rev. **C77**, 065206 (2008), arXiv:0711.0159 [hep-ph].
[22] A. Capella, A. Kaidalov, C. Merino, and J. Tran Thanh Van, Phys.Lett. **B337**, 358 (1994), arXiv:hep-ph/9405338 [hep-ph].
[23] A. Sibirtsev, P. G. Blunden, W. Melnitchouk, and A. W. Thomas, Phys.Rev. **D82**, 013011 (2010), arXiv:1002.0740 [hep-ph].
[24] C. Boros and A. W. Thomas, Phys.Rev. **D60**, 074017 (1999), arXiv:hep-ph/9902372 [hep-ph].
[25] R. Horsley et al., Phys.Rev. **D83**, 051501 (2011), arXiv:1012.0215 [hep-lat].
[26] I. C. Cloët, R. Horsley, J. T. Londergan, Y. Nakamura, D. Pleiter, et al., Phys.Lett. **B714**, 97 (2012), arXiv:1204.3492 [hep-lat].
[27] P. E. Shanahan, A. W. Thomas, and R. D. Young, Phys. Rev. D 87, **094515** (2013), arXiv:1303.4806 [nucl-th].
[28] W. Melnitchouk, R. Ent, and C. Keppel, Phys.Rept. **406**, 127 (2005), arXiv:hep-ph/0501217 [hep-ph].
[29] B. C. Rislow and C. E. Carlson, Phys.Rev. **D83**, 113007 (2011), arXiv:1011.2397 [hep-ph].
[30] M. Gorchtein, C. J. Horowitz, and M. J. Ramsey-Musolf, Phys.Rev. **C84**, 015502 (2011), arXiv:1102.3910 [nucl-th].
[31] N. L. Hall, P. G. Blunden, W. Melnitchouk, A. W. Thomas, and R. D. Young, Phys.Rev. **D88**, 013011 (2013), arXiv:1304.7877 [nucl-th].
[32] C. E. Carlson and M. Vanderhaeghen, Phys.Rev. **A84**, 020102 (2011), arXiv:1101.5965 [hep-ph].

[33] R. J. Hill and G. Paz, Phys.Rev.Lett. **107**, 160402 (2011), arXiv:1103.4617 [hep-ph].
[34] M. C. Birse and J. A. McGovern, Eur.Phys.J. **A48**, 120 (2012), arXiv:1206.3030 [hep-ph].
[35] R. Pohl et al., Nature **466**, 213 (2010).
[36] R. Pohl, R. Gilman, G. A. Miller, and K. Pachucki, Ann.Rev.Nucl.Part.Sci. **63**, 175 (2013), arXiv:1301.0905 [physics.atom-ph].
[37] J. Bernabeu and R. Tarrach, Annals Phys. **102**, 323 (1976).
[38] H. W. Grießhammer, J. A. McGovern, D. R. Phillips, and G. Feldman, Prog.Part.Nucl.Phys. **67**, 841 (2012), arXiv:1203.6834 [nucl-th].
[39] J. C. Collins, Nucl.Phys. **B149**, 90 (1979).
[40] P. E. Shanahan, A. W. Thomas, and R. D. Young, PoS **LATTICE2012**, 165 (2012), arXiv:1301.3231 [hep-lat].
[41] P. E. Shanahan, A. W. Thomas, and R. D. Young, Phys.Rev. **D87**, 074503 (2013), arXiv:1205.5365 [nucl-th].
[42] V. Bernard, N. Kaiser, J. Kambor, and U.-G. Meißner, Phys.Rev. **D46**, 2756 (1992).
[43] C. Gobbi, C. L. Schat, and N. N. Scoccola, Nucl.Phys. **A598**, 318 (1996), arXiv:hep-ph/9509211 [hep-ph].
[44] Y. Tanushi, S. Saito, and M. Uehara, Phys.Rev. **C61**, 055204 (2000), arXiv:nucl-th/9911071 [nucl-th].
[45] A. Aleksejevs and S. Barkanova, J.Phys. **G38**, 035004 (2011), arXiv:1010.3457 [nucl-th].
[46] F. X. Lee, L. Zhou, W. Wilcox, and J. C. Christensen, Phys.Rev. **D73**, 034503 (2006), arXiv:hep-lat/0509065 [hep-lat].
[47] S. Borsanyi, S. Durr, Z. Fodor, C. Hoelbling, S. Katz, et al. (2014), arXiv:1406.4088 [hep-lat].